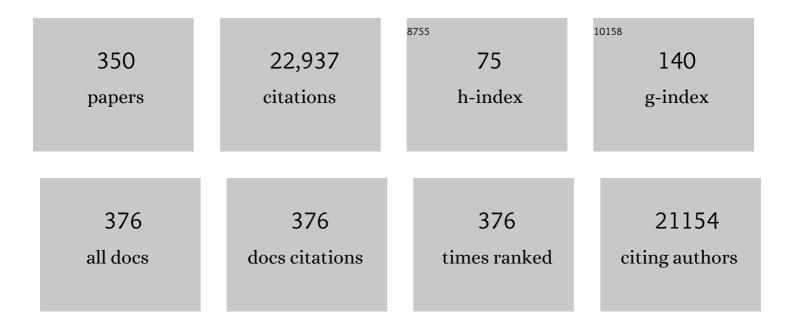
List of Publications by Year in descending order

Source: https://exaly.com/author-pdf/1675695/publications.pdf Version: 2024-02-01



KEWELCHEN

#	Article	IF	CITATIONS
1	Preclinical Evidence of Alzheimer's Disease in Persons Homozygous for the ε4 Allele for Apolipoprotein E. New England Journal of Medicine, 1996, 334, 752-758.	27.0	1,320
2	Functional brain abnormalities in young adults at genetic risk for late-onset Alzheimer's dementia. Proceedings of the National Academy of Sciences of the United States of America, 2004, 101, 284-289.	7.1	907
3	Thermosensory activation of insular cortex. Nature Neuroscience, 2000, 3, 184-190.	14.8	883
4	Fibrillar amyloid-β burden in cognitively normal people at 3 levels of genetic risk for Alzheimer's disease. Proceedings of the National Academy of Sciences of the United States of America, 2009, 106, 6820-6825.	7.1	700
5	Neural correlates of heart rate variability during emotion. NeuroImage, 2009, 44, 213-222.	4.2	588
6	Neuroanatomical correlates of hunger and satiation in humans using positron emission tomography. Proceedings of the National Academy of Sciences of the United States of America, 1999, 96, 4569-4574.	7.1	549
7	The Alzheimer's Disease Neuroimaging Initiative positron emission tomography core. Alzheimer's and Dementia, 2010, 6, 221-229.	0.8	464
8	Brain abnormalities in human obesity: A voxel-based morphometric study. NeuroImage, 2006, 31, 1419-1425.	4.2	459
9	Brain imaging and fluid biomarker analysis in young adults at genetic risk for autosomal dominant Alzheimer's disease in the presenilin 1 E280A kindred: a case-control study. Lancet Neurology, The, 2012, 11, 1048-1056.	10.2	450
10	Declining brain activity in cognitively normal apolipoprotein E ɛ4 heterozygotes: A foundation for using positron emission tomography to efficiently test treatments to prevent Alzheimer's disease. Proceedings of the National Academy of Sciences of the United States of America, 2001, 98, 3334-3339.	7.1	444
11	Longitudinal PET Evaluation of Cerebral Metabolic Decline in Dementia: A Potential Outcome Measure in Alzheimer's Disease Treatment Studies. American Journal of Psychiatry, 2002, 159, 738-745.	7.2	437
12	Correlations between apolipoprotein E ε4 gene dose and brain-imaging measurements of regional hypometabolism. Proceedings of the National Academy of Sciences of the United States of America, 2005, 102, 8299-8302.	7.1	366
13	Using Positron Emission Tomography and Florbetapir F 18 to Image Cortical Amyloid in Patients With Mild Cognitive Impairment or Dementia Due to Alzheimer Disease. Archives of Neurology, 2011, 68, 1404.	4.5	310
14	Alzheimer's Prevention Initiative: A Plan to Accelerate the Evaluation of Presymptomatic Treatments. Journal of Alzheimer's Disease, 2011, 26, 321-329.	2.6	309
15	Arithmetic processing in the brain shaped by cultures. Proceedings of the National Academy of Sciences of the United States of America, 2006, 103, 10775-10780.	7.1	306
16	Noninvasive Quantification of the Cerebral Metabolic Rate for Glucose Using Positron Emission Tomography, 18F-Fluoro-2-Deoxyglucose, the Patlak Method, and an Image-Derived Input Function. Journal of Cerebral Blood Flow and Metabolism, 1998, 18, 716-723.	4.3	286
17	Learning brain connectivity of Alzheimer's disease by sparse inverse covariance estimation. Neurolmage, 2010, 50, 935-949.	4.2	280
18	Measurement of Longitudinal β-Amyloid Change with ¹⁸ F-Florbetapir PET and Standardized Uptake Value Ratios. Journal of Nuclear Medicine, 2015, 56, 567-574.	5.0	273

#	Article	IF	CITATIONS
19	Categorical and correlational analyses of baseline fluorodeoxyglucose positron emission tomography images from the Alzheimer's Disease Neuroimaging Initiative (ADNI). NeuroImage, 2009, 45, 1107-1116.	4.2	258
20	Image-Derived Input Function for Brain PET Studies: Many Challenges and Few Opportunities. Journal of Cerebral Blood Flow and Metabolism, 2011, 31, 1986-1998.	4.3	246
21	Activation of brain regions vulnerable to Alzheimer's disease: The effect of mild cognitive impairment. Neurobiology of Aging, 2006, 27, 1604-1612.	3.1	228
22	Association of CR1, CLU and PICALM with Alzheimer's disease in a cohort of clinically characterized and neuropathologically verified individuals. Human Molecular Genetics, 2010, 19, 3295-3301.	2.9	223
23	Brain Differences in Infants at Differential Genetic Risk for Late-Onset Alzheimer Disease. JAMA Neurology, 2014, 71, 11.	9.0	221
24	Florbetapir PET analysis of amyloid-β deposition in the presenilin 1 E280A autosomal dominant Alzheimer's disease kindred: a cross-sectional study. Lancet Neurology, The, 2012, 11, 1057-1065.	10.2	209
25	Apolipoprotein E Îμ4 and age effects on florbetapir positron emission tomography in healthy aging and Alzheimer disease. Neurobiology of Aging, 2013, 34, 1-12.	3.1	208
26	Successful dieters have increased neural activity in cortical areas involved in the control of behavior. International Journal of Obesity, 2007, 31, 440-448.	3.4	204
27	Resting-state BOLD networks versus task-associated functional MRI for distinguishing Alzheimer's disease risk groups. Neurolmage, 2009, 47, 1678-1690.	4.2	201
28	Interpreting scan data acquired from multiple scanners: A study with Alzheimer's disease. NeuroImage, 2008, 39, 1180-1185.	4.2	200
29	The Alzheimer's Disease Neuroimaging Initiative 2 PET Core: 2015. Alzheimer's and Dementia, 2015, 11, 757-771.	0.8	199
30	Effect of Satiation on Brain Activity in Obese and Lean Women. Obesity, 2001, 9, 676-684.	4.0	184
31	Altered default mode network connectivity in alzheimer's disease—A resting functional MRI and bayesian network study. Human Brain Mapping, 2011, 32, 1868-1881.	3.6	172
32	Tau Positron-Emission Tomography in Former National Football League Players. New England Journal of Medicine, 2019, 380, 1716-1725.	27.0	165
33	Cerebral blood flow in Alzheimer's disease. Vascular Health and Risk Management, 2012, 8, 599.	2.3	162
34	Persistence of abnormal neural responses to a meal in postobese individuals. International Journal of Obesity, 2004, 28, 370-377.	3.4	159
35	Neuroimaging and Obesity. Annals of the New York Academy of Sciences, 2002, 967, 389-397.	3.8	159
36	Less activation of the left dorsolateral prefrontal cortex in response to a meal: a feature of obesity. American Journal of Clinical Nutrition, 2006, 84, 725-731.	4.7	151

#	Article	IF	CITATIONS
37	Association between trait emotional awareness and dorsal anterior cingulate activity during emotion is arousal-dependent. NeuroImage, 2008, 41, 648-655.	4.2	151
38	Twelve-month metabolic declines in probable Alzheimer's disease and amnestic mild cognitive impairment assessed using an empirically pre-defined statistical region-of-interest: Findings from the Alzheimer's Disease Neuroimaging Initiative. NeuroImage, 2010, 51, 654-664.	4.2	145
39	Associations Between Biomarkers and Age in the Presenilin 1 E280A Autosomal Dominant Alzheimer Disease Kindred. JAMA Neurology, 2015, 72, 316.	9.0	145
40	Characterizing Alzheimer's disease using a hypometabolic convergence index. NeuroImage, 2011, 56, 52-60.	4.2	144
41	Genetic Susceptibility for Alzheimer Disease Neuritic Plaque Pathology. JAMA Neurology, 2013, 70, 1150.	9.0	143
42	Sensory experience of food and obesity: a positron emission tomography study of the brain regions affected by tasting a liquid meal after a prolonged fast. NeuroImage, 2005, 24, 436-443.	4.2	139
43	Clinical and multimodal biomarker correlates of ADNI neuropathological findings. Acta Neuropathologica Communications, 2013, 1, 65.	5.2	138
44	Association Between Amyloid and Tau Accumulation in Young Adults With Autosomal Dominant Alzheimer Disease. JAMA Neurology, 2018, 75, 548.	9.0	137
45	A phase Ib multiple ascending dose study of the safety, tolerability, and central nervous system availability of AZD0530 (saracatinib) in Alzheimer's disease. Alzheimer's Research and Therapy, 2015, 7, 35.	6.2	129
46	Voxel-based assessment of gray and white matter volumes in Alzheimer's disease. Neuroscience Letters, 2010, 468, 146-150.	2.1	128
47	Ushering in the study and treatment of preclinical Alzheimer disease. Nature Reviews Neurology, 2013, 9, 371-381.	10.1	125
48	Posterior Cingulate Glucose Metabolism, Hippocampal Glucose Metabolism, and Hippocampal Volume in Cognitively Normal, Late-Middle-Aged Persons at 3 Levels of Genetic Risk for Alzheimer Disease. JAMA Neurology, 2013, 70, 320.	9.0	123
49	Improved Power for Characterizing Longitudinal Amyloid-β PET Changes and Evaluating Amyloid-Modifying Treatments with a Cerebral White Matter Reference Region. Journal of Nuclear Medicine, 2015, 56, 560-566.	5.0	122
50	Sex differences in the human brain's response to hunger and satiation. American Journal of Clinical Nutrition, 2002, 75, 1017-1022.	4.7	120
51	Less activation in the left dorsolateral prefrontal cortex in the reanalysis of the response to a meal in obese than in lean women and its association with successful weight loss. American Journal of Clinical Nutrition, 2007, 86, 573-579.	4.7	113
52	Age-related networks of regional covariance in MRI gray matter: Reproducible multivariate patterns in healthy aging. NeuroImage, 2010, 49, 1750-1759.	4.2	113
53	Postprandial glucagon-like peptide-1 (GLP-1) response is positively associated with changes in neuronal activity of brain areas implicated in satiety and food intake regulation in humans. NeuroImage, 2007, 35, 511-517.	4.2	112
54	Subjective cognitive decline: Self and informant comparisons. Alzheimer's and Dementia, 2014, 10, 93-98.	0.8	111

#	Article	IF	CITATIONS
55	Attentionâ€related networks in Alzheimer's disease: A resting functional MRI study. Human Brain Mapping, 2012, 33, 1076-1088.	3.6	110
56	An empirically derived composite cognitive test score with improved power to track and evaluate treatments for preclinical Alzheimer's disease. Alzheimer's and Dementia, 2014, 10, 666-674.	0.8	110
57	Blood pressure is associated with higher brain amyloid burden and lower glucose metabolism in healthy late middle-age persons. Neurobiology of Aging, 2012, 33, 827.e11-827.e19.	3.1	109
58	Amyloid positron emission tomography and cerebrospinal fluid results from a crenezumab anti-amyloid-beta antibody double-blind, placebo-controlled, randomized phase II study in mild-to-moderate Alzheimer's disease (BLAZE). Alzheimer's Research and Therapy, 2018, 10, 96.	6.2	109
59	Characterization of the image-derived carotid artery input function using independent component analysis for the quantitation of [18F] fluorodeoxyglucose positron emission tomography images. Physics in Medicine and Biology, 2007, 52, 7055-7071.	3.0	107
60	The Alzheimer's Prevention Initiative Autosomalâ€Dominant Alzheimer's Disease Trial: A study of crenezumab versus placebo in preclinical <i>PSEN1</i> E280A mutation carriers to evaluate efficacy and safety in the treatment of autosomalâ€dominant Alzheimer's disease, including a placeboâ€treated noncarrier cohort. Alzheimer's and Dementia: Translational Research and Clinical Interventions, 2018,	3.7	107
61	4 , 150-160. Effect of AZD0530 on Cerebral Metabolic Decline in Alzheimer Disease. JAMA Neurology, 2019, 76, 1219.	9.0	107
62	A rat brain MRI template with digital stereotaxic atlas of fine anatomical delineations in paxinos space and its automated application in voxelâ€wise analysis. Human Brain Mapping, 2013, 34, 1306-1318.	3.6	105
63	Correlations Between Apolipoprotein E ε4 Gene Dose and Whole Brain Atrophy Rates. American Journal of Psychiatry, 2007, 164, 916-921.	7.2	104
64	Evidence for an association between KIBRA and late-onset Alzheimer's disease. Neurobiology of Aging, 2010, 31, 901-909.	3.1	100
65	A 36-week multicenter, randomized, double-blind, placebo-controlled, parallel-group, phase 3 clinical trial of sodium oligomannate for mild-to-moderate Alzheimer's dementia. Alzheimer's Research and Therapy, 2021, 13, 62.	6.2	99
66	Brain Imaging and Blood Biomarker Abnormalities in Children With Autosomal Dominant Alzheimer Disease. JAMA Neurology, 2015, 72, 912.	9.0	94
67	Correlating Cerebral Hypometabolism With Future Memory Decline in Subsequent Converters to Amnestic Pre–Mild Cognitive Impairment. Archives of Neurology, 2008, 65, 1231-6.	4.5	91
68	Hypometabolism in Alzheimer-Affected Brain Regions in Cognitively Healthy Latino Individuals Carrying the Apolipoprotein E ε4 Allele. Archives of Neurology, 2010, 67, 462-8.	4.5	89
69	Neuroimaging and obesity: mapping the brain responses to hunger and satiation in humans using positron emission tomography. Annals of the New York Academy of Sciences, 2002, 967, 389-97.	3.8	87
70	A Multi-Center Randomized Proof-of-Concept Clinical Trial Applying [18F]FDG-PET for Evaluation of Metabolic Therapy with Rosiglitazone XR in Mild to Moderate Alzheimer's Disease. Journal of Alzheimer's Disease, 2011, 22, 1241-1256.	2.6	86
71	Higher serum glucose levels are associated with cerebral hypometabolism in Alzheimer regions. Neurology, 2013, 80, 1557-1564.	1.1	83
72	Gender Differences in Alzheimer Disease: Brain Atrophy, Histopathology Burden, and Cognition. Journal of Neuropathology and Experimental Neurology, 2016, 75, 748-754.	1.7	82

#	Article	IF	CITATIONS
73	Gray matter network associated with risk for Alzheimer's disease in young to middle-aged adults. Neurobiology of Aging, 2012, 33, 2723-2732.	3.1	81
74	Antidepressant effects of sertraline associated with volume increases in dorsolateral prefrontal cortex. Journal of Affective Disorders, 2013, 146, 414-419.	4.1	80
75	Summary Metrics to Assess Alzheimer Disease–Related Hypometabolic Pattern with ¹⁸ F-FDG PET: Head-to-Head Comparison. Journal of Nuclear Medicine, 2012, 53, 592-600.	5.0	79
76	Age-Related Regional Network of Magnetic Resonance Imaging Gray Matter in the Rhesus Macaque. Journal of Neuroscience, 2008, 28, 2710-2718.	3.6	78
77	An evaluation of the algorithms for determining local cerebral metabolic rates of glucose using positron emission tomography dynamic data. IEEE Transactions on Medical Imaging, 1995, 14, 697-710.	8.9	77
78	Accurate measurement of brain changes in longitudinal MRI scans using tensor-based morphometry. NeuroImage, 2011, 57, 5-14.	4.2	77
79	Neuronal injury biomarkers and prognosis in ADNI subjects with normal cognition. Acta Neuropathologica Communications, 2014, 2, 26.	5.2	77
80	Heterogeneous data fusion for alzheimer's disease study. , 2008, , .		75
81	Prevalence of and Potential Risk Factors for Mild Cognitive Impairment in Communityâ€Đwelling Residents of Beijing. Journal of the American Geriatrics Society, 2013, 61, 2111-2119.	2.6	75
82	The Alzheimer's Prevention Initiative Composite Cognitive Test Score. Journal of Clinical Psychiatry, 2014, 75, 652-660.	2.2	75
83	Regional network of magnetic resonance imaging gray matter volume in healthy aging. NeuroReport, 2006, 17, 951-956.	1.2	74
84	Relationships between plasma leptin concentrations and human brain structure: A voxel-based morphometric study. Neuroscience Letters, 2007, 412, 248-253.	2.1	72
85	Altered Connectivity Pattern of Hubs in Default-Mode Network with Alzheimer's Disease: An Granger Causality Modeling Approach. PLoS ONE, 2011, 6, e25546.	2.5	71
86	Functional brain mapping using positron emission tomography scanning in preoperative neurosurgical planning for pediatric brain tumors. Journal of Neurosurgery, 1999, 91, 797-803.	1.6	70
87	Multi-modality sparse representation-based classification for Alzheimer's disease and mild cognitive impairment. Computer Methods and Programs in Biomedicine, 2015, 122, 182-190.	4.7	70
88	Regions of the human brain affected during a liquid-meal taste perception in the fasting state: a positron emission tomography study. American Journal of Clinical Nutrition, 1999, 70, 806-810.	4.7	67
89	Sensitivity to change and prediction of global change for the Alzheimer's Questionnaire. Alzheimer's Research and Therapy, 2015, 7, 1.	6.2	67
90	Prediction of Mild Cognitive Impairment Conversion Using a Combination of Independent Component Analysis and the Cox Model. Frontiers in Human Neuroscience, 2017, 11, 33.	2.0	66

#	Article	IF	CITATIONS
91	Linking functional and structural brain images with multivariate network analyses: A novel application of the partial least square method. NeuroImage, 2009, 47, 602-610.	4.2	65
92	Clustering huge data sets for parametric PET imaging. BioSystems, 2003, 71, 81-92.	2.0	64
93	Left lateralized cerebral glucose metabolism declines in amyloid-β positive persons with mild cognitive impairment. Neurolmage: Clinical, 2018, 20, 286-296.	2.7	64
94	Tracking Alzheimer's disease in transgenic mice using fluorodeoxyglucose autoradiography. NeuroReport, 2000, 11, 987-991.	1.2	63
95	Prediction of Progressive Mild Cognitive Impairment by Multi-Modal Neuroimaging Biomarkers. Journal of Alzheimer's Disease, 2016, 51, 1045-1056.	2.6	62
96	Use of Positron Emission Tomography for Presurgical Localization of Eloquent Brain Areas in Children with Seizures. Pediatric Neurosurgery, 1997, 26, 144-156.	0.7	61
97	Higher serum total cholesterol levels in late middle age are associated with glucose hypometabolism in brain regions affected by Alzheimer's disease and normal aging. Neurolmage, 2010, 49, 169-176.	4.2	61
98	Disrupted Functional and Structural Networks in Cognitively Normal Elderly Subjects with the APOE ɛ4 Allele. Neuropsychopharmacology, 2015, 40, 1181-1191.	5.4	60
99	Florbetapir PET, FDG PET, and MRI in Down syndrome individuals with and without Alzheimer's dementia. Alzheimer's and Dementia, 2015, 11, 994-1004.	0.8	58
100	Prevalence of the apolipoprotein E ε4 allele in amyloid β positive subjects across the spectrum of Alzheimer's disease. Alzheimer's and Dementia, 2018, 14, 913-924.	0.8	58
101	Medial temporal lobe activation during episodic encoding and retrieval: A PET study. , 1999, 9, 575-581.		55
102	Optimal image sampling schedule: a new effective way to reduce dynamic image storage space and functional image processing time. IEEE Transactions on Medical Imaging, 1996, 15, 710-719.	8.9	54
103	A Sparse Structure Learning Algorithm for Gaussian Bayesian Network Identification from High-Dimensional Data. IEEE Transactions on Pattern Analysis and Machine Intelligence, 2013, 35, 1328-1342.	13.9	54
104	The positive impacts of early-life education on cognition, leisure activity, and brain structure in healthy aging. Aging, 2019, 11, 4923-4942.	3.1	54
105	Cortical sources of resting state EEG rhythms are related to brain hypometabolism in subjects with Alzheimer's disease: an EEG-PET study. Neurobiology of Aging, 2016, 48, 122-134.	3.1	53
106	Are We Addicted to Food?. Obesity, 2003, 11, 493-495.	4.0	52
107	A Preliminary Fluorodeoxyglucose Positron Emission Tomography Study in Healthy Adults Reporting Dream-Enactment Behavior. Sleep, 2006, 29, 927-933.	1.1	51
108	Positron Emission Tomography and Neuropathologic Estimates of Fibrillar Amyloid-β in a Patient With Down Syndrome and Alzheimer Disease. Archives of Neurology, 2011, 68, 1461.	4.5	51

#	Article	lF	CITATIONS
109	Diagnostic accuracy of markers for prodromal Alzheimer's disease in independent clinical series. Alzheimer's and Dementia, 2013, 9, 677-686.	0.8	51
110	A Statistical Parametric Mapping Toolbox Used for Voxel-Wise Analysis of FDG-PET Images of Rat Brain. PLoS ONE, 2014, 9, e108295.	2.5	51
111	Large-scale directional connections among multi resting-state neural networks in human brain: A functional MRI and Bayesian network modeling study. NeuroImage, 2011, 56, 1035-1042.	4.2	49
112	Generalized linear least squares method for fast generation of myocardial blood flow parametric images with N-13 ammonia PET. IEEE Transactions on Medical Imaging, 1998, 17, 236-243.	8.9	48
113	Visceral adipose tissue is not increased in Pima Indians compared with equally obese Caucasians and is not related to insulin action or secretion. Diabetologia, 1999, 42, 28-34.	6.3	48
114	An automated algorithm for the computation of brain volume change from sequential MRIs using an iterative principal component analysis and its evaluation for the assessment of whole-brain atrophy rates in patients with probable Alzheimer's disease. NeuroImage, 2004, 22, 134-143.	4.2	48
115	Neuritic and Diffuse Plaque Associations with Memory in Non-Cognitively Impaired Elderly. Journal of Alzheimer's Disease, 2016, 53, 1641-1652.	2.6	48
116	Polymorphism of brain derived neurotrophic factor influences β amyloid load in cognitively intact apolipoprotein E Îμ4 carriers. Neurolmage: Clinical, 2013, 2, 512-520.	2.7	47
117	Whole brain atrophy rate predicts progression from MCI to Alzheimer's disease. Neurobiology of Aging, 2010, 31, 1601-1605.	3.1	45
118	Fat-free body mass but not fat mass is associated with reduced gray matter volume of cortical brain regions implicated in autonomic and homeostatic regulation. NeuroImage, 2013, 64, 712-721.	4.2	45
119	Quantitative Amyloid Imaging in Autosomal Dominant Alzheimer's Disease: Results from the DIAN Study Group. PLoS ONE, 2016, 11, e0152082.	2.5	45
120	Identification and validation of effective connectivity networks in functional magnetic resonance imaging using switching linear dynamic systems. NeuroImage, 2010, 52, 1027-1040.	4.2	43
121	Accelerated functional brain aging in pre-clinical familial Alzheimer's disease. Nature Communications, 2021, 12, 5346.	12.8	43
122	Memory, executive, and multidomain subtle cognitive impairment. Neurology, 2015, 85, 144-153.	1.1	42
123	Studying ventricular abnormalities in mild cognitive impairment with hyperbolic Ricci flow and tensor-based morphometry. NeuroImage, 2015, 104, 1-20.	4.2	42
124	Structural Brain Network Changes across the Adult Lifespan. Frontiers in Aging Neuroscience, 2017, 9, 275.	3.4	42
125	Effects of size and orientation change on hippocampal activation during episodic recognition. NeuroReport, 1997, 8, 3993-3998.	1.2	41
126	Pro-inflammatory cytokine network in peripheral inflammation response to cerebral ischemia. Neuroscience Letters, 2013, 548, 4-9.	2.1	41

#	Article	IF	CITATIONS
127	Machine Learning Approaches for the Neuroimaging Study of Alzheimer's Disease. Computer, 2011, 44, 99-101.	1.1	40
128	Multi-feature kernel discriminant dictionary learning for face recognition. Pattern Recognition, 2017, 66, 404-411.	8.1	40
129	Applying surface-based hippocampal morphometry to study APOE-E4 allele dose effects in cognitively unimpaired subjects. NeuroImage: Clinical, 2019, 22, 101744.	2.7	40
130	Tasting a liquid meal after a prolonged fast is associated with preferential activation of the left hemisphere. NeuroReport, 2002, 13, 1141-1145.	1.2	39
131	Cerebral asymmetry in children when reading Chinese characters. Cognitive Brain Research, 2005, 24, 206-214.	3.0	39
132	Overfeeding Over 24 Hours Does Not Activate Brown Adipose Tissue in Humans. Journal of Clinical Endocrinology and Metabolism, 2013, 98, E1956-E1960.	3.6	39
133	Alterations of Directional Connectivity among Resting-State Networks in Alzheimer Disease. American Journal of Neuroradiology, 2013, 34, 340-345.	2.4	39
134	A Triple Network Connectivity Study of Large-Scale Brain Systems in Cognitively Normal APOE4 Carriers. Frontiers in Aging Neuroscience, 2016, 8, 231.	3.4	39
135	Multimodal Classification of Mild Cognitive Impairment Based on Partial Least Squares. Journal of Alzheimer's Disease, 2016, 54, 359-371.	2.6	39
136	Disrupted White Matter Network and Cognitive Decline in Type 2 Diabetes Patients. Journal of Alzheimer's Disease, 2016, 53, 185-195.	2.6	39
137	Improving tissue segmentation of human brain MRI through preprocessing by the Gegenbauer reconstruction method. NeuroImage, 2003, 20, 489-502.	4.2	38
138	An input function estimation method for FDG-PET human brain studies. Nuclear Medicine and Biology, 2007, 34, 483-492.	0.6	38
139	The value of positron emission tomography and proliferation index in predicting progression in low-grade astrocytomas of childhood. Journal of Neuro-Oncology, 2009, 95, 239-245.	2.9	38
140	Multiple neural networks supporting a semantic task: An fMRI study using independent component analysis. NeuroImage, 2009, 45, 1347-1358.	4.2	38
141	Positron Emission Tomography in Children With Neurofibromatosis-1. Journal of Child Neurology, 1997, 12, 499-506.	1.4	37
142	Mining brain region connectivity for alzheimer's disease study via sparse inverse covariance estimation. , 2009, , .		37
143	Correlations between FDG PET glucose uptake-MRI gray matter volume scores and apolipoprotein E ε4 gene dose in cognitively normal adults: A cross-validation study using voxel-based multi-modal partial least squares. NeuroImage, 2012, 60, 2316-2322.	4.2	36
144	Network analysis of single-subject fMRI during a finger opposition task. NeuroImage, 2006, 32, 325-332.	4.2	35

#	Article	IF	CITATIONS
145	Association of White Matter Integrity and Cognitive Functions in Patients With Subcortical Silent Lacunar Infarcts. Stroke, 2015, 46, 1123-1126.	2.0	35
146	Effects of Image Resolution on Autoradiographic Measurements of Posterior Cingulate Activity in PDAPP Mice: Implications for Functional Brain Imaging Studies of Transgenic Mouse Models of Alzheimer's Disease. NeuroImage, 2002, 16, 1-6.	4.2	33
147	Brain development in Chinese children and adolescents: a structural MRI study. NeuroReport, 2007, 18, 875-880.	1.2	33
148	Higher CSF sTREM2 attenuates ApoE4-related risk for cognitive decline and neurodegeneration. Molecular Neurodegeneration, 2020, 15, 57.	10.8	33
149	An fMRI Study of the Neural Systems Involved in Visually Cued Auditory Top-Down Spatial and Temporal Attention. PLoS ONE, 2012, 7, e49948.	2.5	33
150	Different Patterns of White Matter Disruption among Amnestic Mild Cognitive Impairment Subtypes: Relationship with Neuropsychological Performance. Journal of Alzheimer's Disease, 2013, 36, 365-376.	2.6	32
151	Reanalysis of the Obesity-Related Attenuation in the Left Dorsolateral Prefrontal Cortex Response to a Satiating Meal Using Gyral Regions-of-Interest. Journal of the American College of Nutrition, 2009, 28, 667-673.	1.8	31
152	Cholesterol-related genetic risk scores are associated with hypometabolism in Alzheimer's-affected brain regions. Neurolmage, 2008, 40, 1214-1221.	4.2	30
153	Multi-modal discriminative dictionary learning for Alzheimer's disease and mild cognitive impairment. Computer Methods and Programs in Biomedicine, 2017, 150, 1-8.	4.7	30
154	Effects of Memantine on Clinical Ratings, Fluorodeoxyglucose Positron Emission Tomography Measurements, and Cerebrospinal Fluid Assays in Patients With Moderate to Severe Alzheimer Dementia. Journal of Clinical Psychopharmacology, 2013, 33, 636-642.	1.4	29
155	Peripheral apoE isoform levels in cognitively normal APOE Îμ3/Îμ4 individuals are associated with regional gray matter volume and cerebral glucose metabolism. Alzheimer's Research and Therapy, 2017, 9, 5.	6.2	29
156	Correlations Between Apolipoprotein E ε4 Gene Dose and Whole Brain Atrophy Rates. American Journal of Psychiatry, 2007, 164, 916.	7.2	29
157	Dynamic image data compression in spatial and temporal domains: theory and algorithm. IEEE Transactions on Information Technology in Biomedicine, 1997, 1, 219-228.	3.2	28
158	Early prevention of cognitive impairment in the community population: The Beijing Aging Brain Rejuvenation Initiative. Alzheimer's and Dementia, 2021, 17, 1610-1618.	0.8	28
159	Structural and Functional Brain Changes in the Default Mode Network in Subtypes of Amnestic Mild Cognitive Impairment. Journal of Geriatric Psychiatry and Neurology, 2014, 27, 188-198.	2.3	27
160	Tracking the decline in cerebral glucose metabolism in persons and laboratory animals at genetic risk for Alzheimer's disease. Clinical Neuroscience Research, 2001, 1, 194-206.	0.8	26
161	Mapping joint grey and white matter reductions in Alzheimer's disease using joint independent component analysis. Neuroscience Letters, 2012, 531, 136-141.	2.1	26
162	White Matter Microstructural Change Contributes to Worse Cognitive Function in Patients With Type 2 Diabetes. Diabetes, 2019, 68, 2085-2094.	0.6	26

#	Article	IF	CITATIONS
163	Striatal amyloid is associated with tauopathy and memory decline in familial Alzheimer's disease. Alzheimer's Research and Therapy, 2019, 11, 17.	6.2	26
164	A concise and persistent feature to study brain restingâ€state network dynamics: Findings from the Alzheimer's Disease Neuroimaging Initiative. Human Brain Mapping, 2019, 40, 1062-1081.	3.6	26
165	Applying sparse coding to surface multivariate tensor-based morphometry to predict future cognitive decline. , 2016, 2016, 646-650.		25
166	Brain effective connectivity modeling for alzheimer's disease by sparse gaussian bayesian network. , 2011, , 931-939.		24
167	Blood Pressure Control in Aging Predicts Cerebral Atrophy Related to Small-Vessel White Matter Lesions. Frontiers in Aging Neuroscience, 2017, 9, 132.	3.4	24
168	Effective Connectivity Modeling for fMRI: Six Issues and Possible Solutions Using Linear Dynamic Systems. Frontiers in Systems Neuroscience, 2011, 5, 104.	2.5	23
169	Subjective memory complaints in preclinical autosomal dominant Alzheimer disease. Neurology, 2017, 89, 1464-1470.	1.1	23
170	Cognitive composite score association with Alzheimer's disease plaque and tangle pathology. Alzheimer's Research and Therapy, 2018, 10, 90.	6.2	23
171	Brain imaging measurements of fibrillar amyloidâ€Ĥ² burden, paired helical filament tau burden, and atrophy in cognitively unimpaired persons with two, one, and no copies of the <i>APOE ε4</i> allele. Alzheimer's and Dementia, 2020, 16, 598-609.	0.8	23
172	Association between GAB2 haplotype and higher glucose metabolism in Alzheimer's disease-affected brain regions in cognitively normal APOEε4 carriers. NeuroImage, 2011, 54, 1896-1902.	4.2	22
173	Lysosomal targeting of phafin1 mediated by Rab7 induces autophagosome formation. Biochemical and Biophysical Research Communications, 2012, 417, 35-42.	2.1	22
174	Dynamic FDG-PET Imaging to Differentiate Malignancies from Inflammation in Subcutaneous and In Situ Mouse Model for Non-Small Cell Lung Carcinoma (NSCLC). PLoS ONE, 2015, 10, e0139089.	2.5	22
175	Classification of Alzheimer's Disease, Mild Cognitive Impairment, and Cognitively Unimpaired Individuals Using Multi-feature Kernel Discriminant Dictionary Learning. Frontiers in Computational Neuroscience, 2017, 11, 117.	2.1	22
176	Age-Related Decline in the Topological Efficiency of the Brain Structural Connectome and Cognitive Aging. Cerebral Cortex, 2020, 30, 4651-4661.	2.9	22
177	Effects of <scp><i>APOE</i></scp> promoter polymorphism on the topological organization of brain structural connectome in nondemented elderly. Human Brain Mapping, 2015, 36, 4847-4858.	3.6	21
178	The Receiver Operational Characteristic for Binary Classification with Multiple Indices and Its Application to the Neuroimaging Study of Alzheimer's Disease. IEEE/ACM Transactions on Computational Biology and Bioinformatics, 2013, 10, 173-180.	3.0	20
179	Disrupted white matter structure underlies cognitive deficit in hypertensive patients. European Radiology, 2016, 26, 2899-2907.	4.5	20
180	A transfer learning approach for network modeling. IIE Transactions, 2012, 44, 915-931.	2.1	19

#	Article	IF	CITATIONS
181	A potential role for the midbrain in integrating fatâ€free mass determined energy needs: An H ₂ ¹⁵ O PET study. Human Brain Mapping, 2015, 36, 2406-2415.	3.6	19
182	Aberrant White Matter Networks Mediate Cognitive Impairment in Patients with Silent Lacunar Infarcts in Basal Ganglia Territory. Journal of Cerebral Blood Flow and Metabolism, 2015, 35, 1426-1434.	4.3	18
183	A Two-Year Treatment of Amnestic Mild Cognitive Impairment using a Compound Chinese Medicine: A Placebo Controlled Randomized Trial. Scientific Reports, 2016, 6, 28982.	3.3	18
184	Disrupted Brain Structural Connectivity: Pathological Interactions Between Genetic APOE ε4 Status and Developed MCI Condition. Molecular Neurobiology, 2017, 54, 6999-7007.	4.0	18
185	Precuneus degeneration in nondemented elderly individuals with <i>APOE</i> ɛ4: Evidence from structural and functional MRI analyses. Human Brain Mapping, 2017, 38, 271-282.	3.6	18
186	Age-Related Regional Network Covariance of Magnetic Resonance Imaging Gray Matter in the Rat. Frontiers in Aging Neuroscience, 2020, 12, 267.	3.4	18
187	Applying surface-based morphometry to study ventricular abnormalities of cognitively unimpaired subjects prior to clinically significant memory decline. NeuroImage: Clinical, 2020, 27, 102338.	2.7	18
188	Braak Stage, Cerebral Amyloid Angiopathy, and Cognitive Decline in Early Alzheimer's Disease. Journal of Alzheimer's Disease, 2020, 74, 189-197.	2.6	18
189	Positron emission tomography imaging of serotonin degeneration and beta-amyloid deposition in late-life depression evaluated with multi-modal partial least squares. Translational Psychiatry, 2021, 11, 473.	4.8	18
190	Applications of Neuroimaging to Disease-Modification Trials in Alzheimer's Disease. Behavioural Neurology, 2009, 21, 129-136.	2.1	17
191	FDG–PET parametric imaging by total variation minimization. Computerized Medical Imaging and Graphics, 2009, 33, 295-303.	5.8	17
192	Imaging systems level consolidation of novel associate memories: A longitudinal neuroimaging study. NeuroImage, 2010, 50, 826-836.	4.2	17
193	Is in vivo amyloid distribution asymmetric in primary progressive aphasia?. Annals of Neurology, 2016, 79, 496-501.	5.3	17
194	Hyperbolic Space Sparse Coding with Its Application on Prediction of Alzheimer's Disease in Mild Cognitive Impairment. Lecture Notes in Computer Science, 2016, 9900, 326-334.	1.3	17
195	Hippocampus morphometry study on pathology-confirmed Alzheimer's disease patients with surface multivariate morphometry statistics. , 2018, 2018, 1555-1559.		17
196	Structural Interactions within the Default Mode Network Identified by Bayesian Network Analysis in Alzheimer's Disease. PLoS ONE, 2013, 8, e74070.	2.5	16
197	A pooling-LiNGAM algorithm for effective connectivity analysis of fMRI data. Frontiers in Computational Neuroscience, 2014, 8, 125.	2.1	15
198	Fibrillar amyloid correlates of preclinical cognitive decline. , 2014, 10, e1-e8.		15

12

#	Article	IF	CITATIONS
199	Structural covariance networks across healthy young adults and their consistency. Journal of Magnetic Resonance Imaging, 2015, 42, 261-268.	3.4	15
200	Inflection Point in Course of Mild Cognitive Impairment: Increased Functional Connectivity of Default Mode Network. Journal of Alzheimer's Disease, 2017, 60, 679-690.	2.6	15
201	Baseline demographic, clinical, and cognitive characteristics of the Alzheimer's Prevention Initiative (API) Autosomalâ€Dominant Alzheimer's Disease Colombia Trial. Alzheimer's and Dementia, 2020, 16, 1023-1030.	0.8	15
202	Relationship between the disrupted topological efficiency of the structural brain connectome and glucose hypometabolism in normal aging. NeuroImage, 2021, 226, 117591.	4.2	15
203	Predicting Brain Amyloid Using Multivariate Morphometry Statistics, Sparse Coding, and Correntropy: Validation in 1,101 Individuals From the ADNI and OASIS Databases. Frontiers in Neuroscience, 2021, 15, 669595.	2.8	15
204	Independent Component Analysis-Based Identification of Covariance Patterns of Microstructural White Matter Damage in Alzheimer's Disease. PLoS ONE, 2015, 10, e0119714.	2.5	15
205	Improved application of independent component analysis to functional magnetic resonance imaging study via linear projection techniques. Human Brain Mapping, 2009, 30, 417-431.	3.6	14
206	Assessing the reliability to detect cerebral hypometabolism in probable Alzheimer's disease and amnestic mild cognitive impairment. Journal of Neuroscience Methods, 2010, 192, 277-285.	2.5	14
207	A method for generating image-derived input function in quantitative 18F-FDG PET study based on the monotonicity of the input and output function curve. Nuclear Medicine Communications, 2012, 33, 362-370.	1.1	14
208	Fast direct estimation of the blood input function and myocardial time activity curve from dynamic SPECT projections via reduction in spatial and temporal dimensions. Medical Physics, 2013, 40, 092503.	3.0	14
209	Alzheimer's disease-related changes in regional spontaneous brain activity levels and inter-region interactions in the default mode network. Brain Research, 2013, 1509, 58-65.	2.2	14
210	Longitudinal white matter and cognitive development in pediatric carriers of the apolipoprotein ε4 allele. NeuroImage, 2020, 222, 117243.	4.2	14
211	Alzheimer Disease Biomarkers as Outcome Measures for Clinical Trials in MCI. Alzheimer Disease and Associated Disorders, 2015, 29, 101-109.	1.3	14
212	Applications of neuroimaging to disease-modification trials in Alzheimer's disease. Behavioural Neurology, 2009, 21, 129-36.	2.1	14
213	Ipsilateral brain deactivation specific to the nondominant hand during simple finger movements. NeuroReport, 2008, 19, 483-486.	1.2	13
214	Postprandial plasma PYY concentrations are associated with increased regional gray matter volume and rCBF declines in caudate nuclei — A combined MRI and H215O PET study. NeuroImage, 2012, 60, 592-600.	4.2	13
215	Association between an Alzheimer's Disease-Related Index and APOE ε4 Gene Dose. PLoS ONE, 2013, 8, e67163.	2.5	13
216	Supervised within-class-similar discriminative dictionary learning for face recognition. Journal of Visual Communication and Image Representation, 2016, 38, 561-572.	2.8	13

#	Article	IF	CITATIONS
217	Static and Dynamic Cognitive Reserve Proxy Measures: Interactions with Alzheimer's Disease Neuropathology and Cognition. , 2017, 07, .		13
218	Plasma Apolipoprotein E3 and Glucose Levels Are Associated in APOE ɛ3/ɛ4 Carriers. Journal of Alzheimer's Disease, 2021, 81, 339-354.	2.6	13
219	Wavelet-Based De-noising of Positron Emission Tomography Scans. Journal of Scientific Computing, 2012, 50, 665-677.	2.3	12
220	The Effects of an APOE Promoter Polymorphism on Human White Matter Connectivity during Non-Demented Aging. Journal of Alzheimer's Disease, 2016, 55, 77-87.	2.6	12
221	Predicting Imminent Progression to Clinically Significant Memory Decline Using Volumetric MRI and FDG PET. Journal of Alzheimer's Disease, 2018, 63, 603-615.	2.6	12
222	White matter hyperintensities are a prominent feature of autosomalÂdominant Alzheimer's disease that emerge prior to dementia. Alzheimer's Research and Therapy, 2022, 14, .	6.2	12
223	Combining Multiple Markers to Improve the Longitudinal Rate of Progression: Application to Clinical Trials on the Early Stage of Alzheimer's Disease. Statistics in Biopharmaceutical Research, 2013, 5, 54-66.	0.8	11
224	Improved Estimation of the Number of Independent Components for Functional Magnetic Resonance Data by a Whitening Filter. IEEE Journal of Biomedical and Health Informatics, 2013, 17, 629-641.	6.3	11
225	A Semi-Automated Region of Interest Detection Method in the Scintigraphic Glomerular Filtration Rate Determination for Patients With Abnormal Low Renal Function. Clinical Nuclear Medicine, 2013, 38, 855-862.	1.3	11
226	<i><scp>SORL</scp>1</i> rs1699102 polymorphism modulates ageâ€related cognitive decline and gray matter volume reduction in nonâ€demented individuals. European Journal of Neurology, 2017, 24, 187-194.	3.3	11
227	Aberrant Connectivity in Mild Cognitive Impairment and Alzheimer Disease Revealed by Multimodal Neuroimaging Data. Neurodegenerative Diseases, 2018, 18, 5-18.	1.4	11
228	<i>APOE</i> influences working memory in nonâ€demented elderly through an interaction with <i>SPON1</i> rs2618516. Human Brain Mapping, 2018, 39, 2859-2867.	3.6	11
229	Interaction Between BDNF Val66Met and APOE4 on Biomarkers of Alzheimer's Disease and Cognitive Decline. Journal of Alzheimer's Disease, 2020, 78, 721-734.	2.6	11
230	New estimation methods that directly use the time accumulated counts in the input function in quantitative dynamic PET studies. Physics in Medicine and Biology, 1994, 39, 2073-2090.	3.0	10
231	A method of generating image-derived input function in a quantitative 18F-FDG PET study based on the shape of the input function curve. Nuclear Medicine Communications, 2011, 32, 1121-1127.	1.1	10
232	Added value and limitations of amyloid-PET imaging: review and analysis of selected cases of mild cognitive impairment and dementia. Neurocase, 2017, 23, 41-51.	0.6	10
233	The Interactive Effects of Age and PICALM rs541458 Polymorphism on Cognitive Performance, Brain Structure, and Function in Non-demented Elderly. Molecular Neurobiology, 2018, 55, 1271-1283.	4.0	10
234	Noninvasive Input Function Acquisition and Simultaneous Estimations With Physiological Parameters for PET Quantification: A Brief Review. IEEE Transactions on Radiation and Plasma Medical Sciences, 2020, 4, 676-683.	3.7	10

#	Article	IF	CITATIONS
235	Developing univariate neurodegeneration biomarkers with low-rank and sparse subspace decomposition. Medical Image Analysis, 2021, 67, 101877.	11.6	10
236	Beijing Aging Brain Rejuvenation Initiative: aging with grace. Scientia Sinica Vitae, 2018, 48, 721-734.	0.3	10
237	Sex differences in cognitive resilience in preclinical autosomalâ€dominant Alzheimer's disease carriers and nonâ€carriers: Baseline findings from the API ADAD Colombia Trial. Alzheimer's and Dementia, 2022, 18, 2272-2282.	0.8	10
238	Deep residual inception encoderâ€decoder network for amyloid PET harmonization. Alzheimer's and Dementia, 2022, 18, 2448-2457.	0.8	10
239	Neural substrates in color processing: A comparison between painting majors and non-majors. Neuroscience Letters, 2011, 487, 191-195.	2.1	9
240	Regional covariance patterns of gray matter alterations in Alzheimer's disease and its replicability evaluation. Journal of Magnetic Resonance Imaging, 2014, 39, 143-149.	3.4	9
241	Regional Neural Response Differences in the Determination of Faces or Houses Positioned in a Wide Visual Field. PLoS ONE, 2013, 8, e72728.	2.5	9
242	Brain structural and functional anomalies associated with simultanagnosia in patients with posterior cortical atrophy. Brain Imaging and Behavior, 2022, 16, 1148-1162.	2.1	9
243	Cerebral Amyloid Angiopathy and Neuritic Plaque Pathology Correlate with Cognitive Decline in Elderly Non-Demented Individuals. Journal of Alzheimer's Disease, 2019, 67, 411-422.	2.6	8
244	PET evidence of preclinical cerebellar amyloid plaque deposition in autosomal dominant Alzheimer's disease-causing Presenilin-1 E280A mutation carriers. NeuroImage: Clinical, 2021, 31, 102749.	2.7	8
245	Accelerated Brain Aging in Amnestic Mild Cognitive Impairment: Relationships with Individual Cognitive Decline, Risk Factors for Alzheimer Disease, and Clinical Progression. Radiology: Artificial Intelligence, 2021, 3, e200171.	5.8	8
246	Glucose metabolism patterns: A potential index to characterize brain ageing and predict high conversion risk into cognitive impairment. GeroScience, 2022, 44, 2319-2336.	4.6	8
247	Decay correction methods in dynamic PET studies. IEEE Transactions on Nuclear Science, 1995, 42, 2173-2179.	2.0	7
248	Improved interâ€modality image registration using normalized mutual information with coarseâ€binned histograms. Communications in Numerical Methods in Engineering, 2009, 25, 583-595.	1.3	7
249	Identifying effective connectivity parameters in simulated fMRI: a direct comparison of switching linear dynamic system, stochastic dynamic causal, and multivariate autoregressive models. Frontiers in Neuroscience, 2013, 7, 70.	2.8	7
250	Longitudinal Changes in Serum Glucose Levels are Associated with Metabolic Changes in Alzheimer's Disease Related Brain Regions. Journal of Alzheimer's Disease, 2018, 62, 833-840.	2.6	7
251	Community-based Model for Dementia Risk Screening: The Beijing Aging Brain Rejuvenation Initiative (BABRI) Brain Health System. Journal of the American Medical Directors Association, 2021, 22, 1500-1506.e3.	2.5	7
252	Separating lexical-semantic access from other mnemonic processes in picture-name verification. Frontiers in Psychology, 2013, 4, 706.	2.1	6

#	Article	IF	CITATIONS
253	Aging Influence on Gray Matter Structural Associations within the Default Mode Network Utilizing Bayesian Network Modeling. Frontiers in Aging Neuroscience, 2014, 6, 105.	3.4	6
254	Visualizing Alzheimer's disease progression in low dimensional manifolds. Heliyon, 2019, 5, e02216.	3.2	6
255	Changes in the Functional and Structural Default Mode Network Across the Adult Lifespan Based on Partial Least Squares. IEEE Access, 2019, 7, 82256-82265.	4.2	6
256	Improved Prediction of Imminent Progression to Clinically Significant Memory Decline Using Surface Multivariate Morphometry Statistics and Sparse Coding. Journal of Alzheimer's Disease, 2021, 81, 209-220.	2.6	6
257	Whole Brain Atrophy and Sample Size Estimate via Iterative Principal Component Analysis for Twelve-month Alzheimer's Disease Trials. Neuroscience and Biomedical Engineering, 2013, 1, 40-47.	0.4	6
258	Reconfigured metabolism brain network in asymptomatic microtubule-associated protein tau mutation carriers: a graph theoretical analysis. Alzheimer's Research and Therapy, 2022, 14, 52.	6.2	6
259	Three Cases of Primary Hyperparathyroidism (PHP) with Prior Failed Surgery Where Culprit Lesions Were Identified by 11C-Methionine Positron Emission Tomography (PET) and Accurately Localized with PET-MRI Coregistration. Molecular Imaging and Biology, 2000, 3, 31-36.	0.3	5
260	Effective connectivity analysis of default mode network based on the Bayesian network learning approach. Proceedings of SPIE, 2009, , .	0.8	5
261	Temporal and instantaneous connectivity of default mode network estimated using Gaussian Bayesian network frameworks. Neuroscience Letters, 2012, 513, 62-66.	2.1	5
262	Characterizing structural association alterations within brain networks in normal aging using Gaussian Bayesian networks. Frontiers in Computational Neuroscience, 2014, 8, 122.	2.1	5
263	Morphometric analysis of hippocampus and lateral ventricle reveals regional difference between cognitively stable and declining persons. , 2016, 2016, 14-18.		5
264	A novel transfer learning model for predictive analytics using incomplete multimodality data. IISE Transactions, 2021, 53, 1010-1022.	2.4	5
265	Disrupted anterior and posterior hippocampal structural networks correlate impaired verbal memory and spatial memory in different subtypes of mild cognitive impairment. European Journal of Neurology, 2021, 28, 3955-3964.	3.3	5
266	APOE ε4 allele accelerates age-related multi-cognitive decline and white matter damage in non-demented elderly. Aging, 2020, 12, 12019-12031.	3.1	5
267	Federated Morphometry Feature Selection for Hippocampal Morphometry Associated Beta-Amyloid and Tau Pathology. Frontiers in Neuroscience, 2021, 15, 762458.	2.8	5
268	Methods for the correction of vascular artifacts in PET O-15 water brain-mapping studies. IEEE Transactions on Nuclear Science, 1996, 43, 3308-3314.	2.0	4
269	Regional myocardial oxygen consumption estimated by carbon-11 acetate and positron emission tomography before and after repetitive ischemiaâ~†â~†â~†â~tâ~ Journal of Nuclear Cardiology, 2000, 7, 228-234.	2.1	4
270	Monte-Carlo based neuroimaging set-level multiple-comparison correction. IFAC Postprint Volumes IPPV / International Federation of Automatic Control, 2003, 36, 11-15.	0.4	4

#	Article	IF	CITATIONS
271	A variant of logistic transfer function in Infomax and a postprocessing procedure for independent component analysis applied to fMRI data. Magnetic Resonance Imaging, 2007, 25, 703-711.	1.8	4
272	Reducing modeling error of graphical methods for estimating volume of distribution measurements in PIB–PET study. Mathematical Biosciences, 2010, 226, 134-146.	1.9	4
273	Statistical considerations for assessing cognition and neuropathology associations in preclinical Alzheimer's disease. Biostatistics and Epidemiology, 2017, 1, 92-104.	0.4	4
274	An 8-week open label trial of l-Threonic Acid Magnesium Salt in patients with mild to moderate dementia. Personalized Medicine in Psychiatry, 2017, 4-6, 7-12.	0.1	4
275	Multistage Grading of Amnestic Mild Cognitive Impairment: The Associated Brain Gray Matter Volume and Cognitive Behavior Characterization. Frontiers in Aging Neuroscience, 2017, 8, 332.	3.4	4
276	A Computational Monte Carlo Simulation Strategy to Determine the Temporal Ordering of Abnormal Age Onset Among Biomarkers of Alzheimer's Disease. IEEE/ACM Transactions on Computational Biology and Bioinformatics, 2022, 19, 2613-2622.	3.0	4
277	Inter-Frame Co-Registration of Dynamically Acquired Fluoro-Deoxyglucose Positron Emission Tomography Human Brain Data. , 2007, , .		3
278	Longitudinal Evaluation of Sympathetic Nervous System and Perfusion in Normal and Spontaneously Hypertensive Rat Hearts with Dynamic Single-Photon Emission Computed Tomography. Molecular Imaging, 2015, 14, 7290.2015.00012.	1.4	3
279	P3â€285: Patchâ€Based Sparse Coding and Multivariate Surface Morphometry for Predicting Amnestic Mild Cognitive Impairment and Alzheimer'S Disease in Cognitively Unimpaired Individuals. Alzheimer's and Dementia, 2016, 12, P947.	0.8	3
280	Combinations of Multiple Neuroimaging Markers using Logistic Regression for Auxiliary Diagnosis of Alzheimer Disease and Mild Cognitive Impairment. Neurodegenerative Diseases, 2018, 18, 91-106.	1.4	3
281	Computing Univariate Neurodegenerative Biomarkers with Volumetric Optimal Transportation: A Pilot Study. Neuroinformatics, 2020, 18, 531-548.	2.8	3
282	New method for the analysis of multiple positron emission tomography dynamic datasets: an example applied to the estimation of the cerebral metabolic rate of oxygen. Medical and Biological Engineering and Computing, 1998, 36, 83-90.	2.8	2
283	Positron Emission Tomography and Magnetic Resonance Imaging in the Study of Cognitively Normal Persons at Differential Genetic Risk for Alzheimer's Dementia. , 2004, , 151-177.		2
284	MRI Template and Atlas Toolbox for the C57BL/6J Mouse Brain. , 2005, , .		2
285	Sparse Inverse Covariance Analysis of human brain for Alzheimer's disease study. , 2009, , .		2
286	Whole brain atrophy based on iterative principal component analysis and MRI techniques in the study of Alzheimer's disease. , 2009, , .		2
287	The application of independent component analysis with projection method to two-task fMRI data over multiple subjects. , 2011, , .		2
288	Comparison of gray matter volume and thickness for analysis of cortical changes in Alzheimer's disease. Proceedings of SPIE, 2011, , .	0.8	2

#	Article	IF	CITATIONS
289	The simulation of land use type change in Erhai Basin based on agent based modeling. , 2011, , .		2
290	Separating 4D multi-task fMRI data of multiple subjects by independent component analysis with projection. Magnetic Resonance Imaging, 2013, 31, 60-74.	1.8	2
291	Cortical thickness across the lifespan in a Colombian cohort with autosomalâ€dominant Alzheimer's disease: A crossâ€sectional study. Alzheimer's and Dementia: Diagnosis, Assessment and Disease Monitoring, 2021, 13, e12233.	2.4	2
292	Predicting future cognitive decline with hyperbolic stochastic coding. Medical Image Analysis, 2021, 70, 102009.	11.6	2
293	Limitations of clinical trial sample size estimate by subtraction of two measurements. Statistics in Medicine, 2022, 41, 1137-1147.	1.6	2
294	An Optimal Transportation based Univariate Neuroimaging Index. Proceedings of the IEEE International Conference on Computer Vision, 2017, 2017, 182-191.	0.0	2
295	Hemispheric Asymmetry and Atypical Lobar Progression of Alzheimer-Type Tauopathy. Journal of Neuropathology and Experimental Neurology, 2022, 81, 158-171.	1.7	2
296	Construction of mouse brain MRI templates using SPM 99. IFAC Postprint Volumes IPPV / International Federation of Automatic Control, 2003, 36, 113-118.	0.4	1
297	A new post-processing method of applying independent component analysis to fMRI data. , 2006, , .		1
298	Regional gray matter abnormalities in patients with schizophrenia determined with optimized voxel-based morphometry. , 2006, , .		1
299	An automated normative-based fluorodeoxyglucose positron emission tomography image-analysis procedure to aid Alzheimer disease diagnosis using statistical parametric mapping and interactive image display. , 2006, 6144, 1638.		1
300	Is the brain representation of hunger normal in the Prader-Willi syndrome?. International Journal of Obesity, 2007, 31, 390-390.	3.4	1
301	An improved exponential filter for fast nonlinear registration of brain magnetic resonance images. Progress in Natural Science: Materials International, 2009, 19, 759-767.	4.4	1
302	Using the Artificial Neural Network to discriminate between normal controls with different APOE e4 genotypes and probable AD cases in PIB-PET studies. , 2009, , .		1
303	Reducing the noise effects in Logan graphic analysis for PET receptor measurements. , 2009, , .		1
304	Mapping gray matter volume and cortical thickness in Alzheimer's disease. , 2010, , .		1
305	Deriving difference between the Bayesian networks based patterns of the effective connectivity using permutation test in fMRI studies. , 2010, , .		1
306	Application of Granger causality analysis to effective connectivity of the default-mode network. , 2010, , .		1

#	Article	IF	CITATIONS
307	Independent component analysis of DTI data reveals white matter covariances in Alzheimer's disease. , 2014, , .		1
308	Design of a short nonuniform acquisition protocol for quantitative analysis in dynamic cardiac SPECT imaging - a retrospective ¹²³ I-MIBG animal study. Medical Physics, 2017, 44, 3639-3649.	3.0	1
309	An Optimal Transportation Based Univariate Neuroimaging Index. , 2017, , .		1
310	Studying APOE É›4 Allele Dose Effects withÂa Univariate Morphometry Biomarker. Journal of Alzheimer's Disease, 2022, 85, 1233-1250.	2.6	1
311	Predicting Tau accumulation in cerebral cortex with multivariate MRI morphometry measurements, sparse coding, and correntropy. , 2021, 12088, .		1
312	Investigating the Effect of Tau Deposition and Apoe on Hippocampal Morphometry in Alzheimer's Disease: A Federated Chow Test Model. , 2022, , .		1
313	<title>Generalized linear least squares method for estimating myocardial blood flow with N-13 ammonia positron emission tomography</title> . , 1996, , .		0
314	Simultaneous analysis of noisy signals obtained from multiple experiments, with application to deriving brain functional images. , 0, , .		0
315	Functional brain mapping using positron emission tomography scanning in preoperative neurosurgical planning for pediatric brain tumors. Neurosurgical Focus, 2000, 8, 1-7.	2.3	0
316	Constructing and assessing brain templates from Chinese pediatric MRI data using SPM. , 2005, , .		0
317	A Monte-Carlo Simulation Package, Multiple Comparison Corrections and Power Estimation Incorporating Secondary Supportive Evidence. , 2007, , .		0
318	Automated diagnosis and prediction of Alzheimer disease using magnetic resonance image. , 2007, , .		0
319	Functional network connectivity analysis based on partial correlation in Alzheimer's disease. , 2009, , .		0
320	Mapping brain development during childhood, adolescence and young adulthood. Proceedings of SPIE, 2009, , .	0.8	0
321	Automation of the Logan plot based PiB-PET quantification over multiple subjects and multiple reference regions. , 2009, , .		0
322	The improvement of ICA with projection technique in multitask fMRI data analysis. Proceedings of SPIE, 2010, , .	0.8	0
323	A resting-state functional MRI study of the post-effect of acupuncture. , 2011, , .		0
324	Primary motor cortex activity reduction under the regulation of SMA by real-time fMRI. , 2012, , .		0

#	Article	IF	CITATIONS
325	Structural correlation in the default mode network in Alzheimer's disease. , 2012, , .		0
326	O2-03-01: Validation of the Alzheimer's Prevention Initiative Composite Cognitive Test Score. , 2013, 9, P320-P320.		0
327	O4-08-01: Association between the Alzheimer's disease-related hypometabolic convergence index and clinical ratings in cognitively normal older adults with and without significant fibrillar amyloid burden: Findings from the Alzheimer's Disease Neuroimaging. , 2013, 9, P698-P698.		0
328	Biomarker Research of Preclinical Alzheimer's Disease and MCI Based on Neuroimage Techniques. Neuroscience and Biomedical Engineering, 2014, 1, 92-101.	0.4	0
329	P4-298: IMPROVING THE POWER TO TRACK FIBRILLAR AMYLOID PET MEASUREMENTS AND EVALUATE AMYLOID-MODIFYING TREATMENTS USING A CEREBRAL WHITE MATTER REFERENCE REGION-OF-INTEREST. , 2014, 10, P894-P894.		Ο
330	P3-169: Reduced default network functional connectivity and verbal learning in cognitively unimpaired late middle-aged and older adults: Exploratory findings from the arizona ApoE cohort study. , 2015, 11, P694-P694.		0
331	Meet Our Editor:. Neuroscience and Biomedical Engineering, 2015, 3, 1-1.	0.4	0
332	P1-292: Lower Frontal Amyloid Burden in Antidepressant Users: Preliminary Findings From Persons With and Without Post-Traumatic Stress Disorder in The ADNI DOD Study. , 2016, 12, P532-P533.		0
333	P2â€243: Higher BMI is Associated with Greater Cerebral Glucose Metabolism in Late Middleâ€Aged and Elderly Subjects Regardless of <i>APOE</i> ε4 Genotype. Alzheimer's and Dementia, 2016, 12, P717.	0.8	0
334	A CAD Tribute to Gerald Farin. CAD Computer Aided Design, 2016, 80, 1-5.	2.7	0
335	[P4–247]: LEFT LATERALIZED CEREBRAL GLUCOSE METABOLISM DECLINES IN AMYLOIDâ€Î²â€POSITIVE SUBJE0 WITH MILD COGNITIVE IMPAIRMENT. Alzheimer's and Dementia, 2017, 13, P1372.	стร ₈	0
336	[ICâ€Pâ€210]: LEFT LATERALIZED CEREBRAL GLUCOSE METABOLISM DECLINES IN AMYLOIDâ€Î²â€" POSITIVE SU WITH MILD COGNITIVE IMPAIRMENT. Alzheimer's and Dementia, 2017, 13, P152.	BIECTS	0
337	Impact statement: Sequential biomarker testing for Alzheimer's disease early diagnosis. IISE Transactions on Healthcare Systems Engineering, 2017, 7, 247-247.	1.7	0
338	[P3–032]: SSRI USE ASSOCIATED WITH REDUCED AMYLOID BURDEN IN PERSONS WITH COMBATâ€RELATED PTSD: PRELIMINARY FINDINGS FROM ADNIâ€DOD. Alzheimer's and Dementia, 2017, 13, P942.	0.8	0
339	[ICâ€Pâ€209]: CAVEATS WHEN SUBTRACTING TWO SERIAL MEASUREMENTS TO ESTIMATE THE NUMBER OF PARTICIPANTS NEEDED FOR CLINICAL TRIALS THAT ARE LONGER OR SHORTER THAN THE OBSERVED MEASUREMENT INTERVAL. Alzheimer's and Dementia, 2017, 13, P151.	0.8	0
340	[ICâ€Pâ€211]: A COMPUTATIONAL MONTE CARLO SIMULATION STRATEGY TO COMPARE THE ONSET OF DIFFER BIOMARKER AND COGNITIVE CHANGES. Alzheimer's and Dementia, 2017, 13, P152.	ENT.	0
341	[P1–260]: A COMPUTATIONAL MONTEâ€CARLO SIMULATION STRATEGY TO COMPARE THE ONSET OF DIFFERE BIOMARKER AND COGNITIVE CHANGES. Alzheimer's and Dementia, 2017, 13, P349.	ENT 0.8	0
342	[P1–261]: TRACKING ALZHEIMER's DISEASE PROGRESSION BY NONâ€LINEAR DIMENSION REDUCTION OF BRA MRI FEATURES. Alzheimer's and Dementia, 2017, 13, P349.	IN 0.8	0

#	Article	IF	CITATIONS
343	[P2–333]: CAVEATS WHEN SUBTRACTING TWO SERIAL MEASUREMENTS TO ESTIMATE THE NUMBER OF PARTICIPANTS NEEDED FOR CLINICAL TRIALS THAT ARE LONGER OR SHORTER THAN THE OBSERVED MEASUREMENT INTERVAL. Alzheimer's and Dementia, 2017, 13, P748.	0.8	0
344	Diagnosis on Mild Cognitive Impairment Patients for Alzheimer Disease with Missing Data. , 2017, , .		0
345	P1â€454: RELATIONSHIPS BETWEEN MEAN CORTICAL AMYLOID BURDEN AND REGIONAL GRAY MATTER REDUCTIONS IN ALZHEIMER'S DEMENTIA, MILD COGNITIVE IMPAIRMENT AND UNIMPAIRED OLDER ADULTS. Alzheimer's and Dementia, 2018, 14, P490.	0.8	0
346	ICâ€Pâ€003: RELATIONSHIPS BETWEEN MEAN CORTICAL AMYLOID BURDEN AND REGIONAL GRAY MATTER REDUCTIONS IN ALZHEIMER'S DEMENTIA, MILD COGNITIVE IMPAIRMENT AND UNIMPAIRED OLDER ADULTS. Alzheimer's and Dementia, 2018, 14, P15.	0.8	0
347	ADMultiImg: a novel missing modality transfer learning based CAD system for diagnosis of MCI due to AD using incomplete multi-modality imaging data. , 2018, , .		0
348	Adaptive smoothing strategies to eliminate the scalp/ventricle artifact in statistical parametric mapping. , 0, , .		0
349	Female-specific effects of the catechol-O-methyl transferase Val158Met gene polymorphism on working memory-related brain function. Aging, 2020, 12, 23900-23916.	3.1	Ο
350	Improved comparability between measurements of mean cortical amyloid plaque burden derived from different PET tracers using multiple regionsâ€ofâ€interest and machine learning. Alzheimer's and Dementia, 2021, 17, .	0.8	0